



Preparation and biological evaluation of ethionamide-mesoporous silicon nanoparticles against *Mycobacterium tuberculosis*



Nuno Vale^{a,*}, Alexandra Correia^b, Sara Silva^a, Patrícia Figueiredo^b, Ermei Mäkilä^c, Jarno Salonen^c, Jouni Hirvonen^b, Jorge Pedrosa^d, Hélder A. Santos^b, Alexandra Fraga^d

^a UCIBIO/REQUIMTE, Department of Chemistry and Biochemistry, Faculty of Sciences, University of Porto, Rua do Campo Alegre, 687, 4169-007 Porto, Portugal

^b Division of Pharmaceutical Chemistry and Technology, Faculty of Pharmacy, University of Helsinki, FI-00014 Helsinki, Finland

^c Laboratory of Industrial Physics, Department of Physics and Astronomy, University of Turku, FI-20014, Finland

^d Microbiology and Infection Research Domain, Life and Health Sciences Research Institute, School of Health Sciences, University of Minho, Campus de Gualtar, 4710-057 Braga, Portugal

ARTICLE INFO

Article history:

Received 15 November 2016

Revised 21 December 2016

Accepted 22 December 2016

Available online 26 December 2016

Keywords:

Ethionamide

Porous silicon nanoparticles

Mycobacterium tuberculosis

Strain H37Rv

MIC₅₀

ABSTRACT

Ethionamide (ETH) is an important second-line antituberculosis drug used for the treatment of patients infected with multidrug-resistant *Mycobacterium tuberculosis*. Recently, we reported that the loading of ETH into thermally carbonized-porous silicon (TCPSi) nanoparticles enhanced the solubility and permeability of ETH at different pH-values and also increased its metabolism process. Based on these results, we synthesized carboxylic acid functionalized thermally hydrocarbonized porous silicon nanoparticles (UnTHCPSi NPs) conjugated with ETH and its antimicrobial effect was evaluated against *Mycobacterium tuberculosis* strain H37Rv. The activity of the conjugate was increased when compared to free-ETH, which suggests that the nature of the synergy between the NPs and ETH is likely due to the weakening of the bacterial cell wall that improves conjugate-penetration. These ETH-conjugated NPs have great potential in reducing dosing frequency of ETH in the treatment of multidrug-resistant tuberculosis (MDR-TB).

© 2016 Elsevier Ltd. All rights reserved.

Tuberculosis (TB) remains a leading cause of death from infectious diseases worldwide. In 2014, 9.6 million people were estimated to have developed active TB and 1.5 million died from the disease, according to the World Health Organization (WHO) report.¹ Adding to this, there has been an increase in the global TB incidence among individuals infected with HIV. From the 9.6 million new cases reported in 2014, 12% were HIV-positive.¹

The emergence of multidrug-resistant (MDR) TB, defined by resistance to both rifampicin (RIF) and isoniazid (INH), also represents a major public health concern in the control of the disease. Indeed, it has been estimated that 480,000 patients developed MDR-TB in 2014.² Given the limited knowledge on relevant mechanisms of drug resistance in TB,³ it is urgent to develop new strategies to improve the bioavailability of anti-TB drugs.

The most effective first-line antibiotics for the treatment of TB include rifampicin and INH.⁴ One of the most widely used second-line drugs for the treatment of MDR-TB is ethionamide (Scheme 1, ETH, **1**), which is a thioamide antibiotic structurally similar to INH. The mode of action of the activated form of ETH is via inhibition of the InhA gene product, enoyl-ACP reduc-

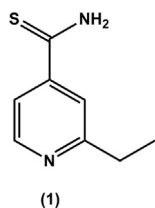
tase,^{5–7} the same target of INH.⁵ ETH is activated by a KatG-independent mechanism⁵ and the major metabolite in vivo is its S-oxide.^{8,9}

The active form of ETH create adducts with nicotinamide adenine dinucleotide (NAD) that inhibit the inhA enzyme⁵ and, consequently, induces disorders on mycolic acid synthesis. Studies both in mammals and bacteria suggest that ETH-SO retains the biological activity of the parent drug,¹⁰ which is in line with the fact that, ETH and many current antimycobacterial agents, require some form of cellular activation corresponding to the oxidative, reductive, or hydrolytic unmasking of active groups.^{11–13} Other metabolites for ETH, such as ETH-nitrite, ETH-aldehyde and ETH-OH, have been identified, although with less therapeutic importance.^{14–18}

Recently, we reported the solubility, toxicity, permeability, and metabolic profiles of thermally carbonized-porous silicon (TCPSi) microparticles loaded with ETH. The solubility and permeability of ETH was clearly enhanced after being loaded into TCPSi particles at different pH-values and showed a fast metabolism process in the presence of the TCPSi particles.¹⁹ Based on these promising results, we synthesized carboxylic acid functionalized thermally hydrocarbonized porous silicon nanoparticles (UnTHCPSi NPs) conjugated with ETH^{20–22} and evaluated the antimicrobial effect of this conjugate against *M. tuberculosis* strain H37Rv,²³ the most

* Corresponding author.

E-mail address: nuno.vale@fc.up.pt (N. Vale).



Scheme 1. Structure of ethionamide (ETH)

commonly used control reference strain in clinical and research laboratory settings.

Delivery systems using PSi nanoparticles (NPs) are known to be superior than microparticles, because they enhance the interactions with the cells and can be uptaken in high extents.^{24–26} The high drug bioavailabilities of PSi NPs may also result in drug protection and controlled drug release when the nanocarriers are exposed to the circulation.^{24–26}

For the synthesis of the UnTHCPSi NPs, monocrystalline boron doped p⁺ Si (100) wafers with a resistivity of 0.01–0.02 Ω·cm were electrochemically anodized in a 1:1 (v/v) hydrofluoric acid (38%)-ethanol electrolyte, pulsed with low and high current density etching profiles to fracture the surface of Si wafers at different intervals. After that, the etching current was increased to the electropolishing region to lift off the obtained multilayer film from the substrate. The membranes were dried and set under N₂ flow (1 L/min) for 30 min at room temperature to eliminate oxygen and residual moisture. Then, at room temperature, acetylene (C₂H₂) flow (1 L/min) was added to the N₂ flow for 15 min before enhancing the temperature for 15 min to 500 °C under the 1:1 (v/v) N₂/C₂H₂ flow. The THCPSi films were then allowed to cool down to room temperature under N₂ flow and further treated by immersion in undecylenic acid for 16 h at 120 °C to provide a carboxyl functionalization (UnTHCPSi). The NPs were made by ball milling the UnTHCPSi films in 10 vol-% undecylenic acid-decane solution.^{21,22}

Table 1

Size, Pdl, ζ-potential of the NPs before and after the ETH conjugation. Results are presented as mean ± SD (n ≥ 3).

NP	Size (nm)	Pdl (polydispersity index)	Zeta (ζ)-potential (mV)
UnTHCPSi	175.91 ± 0.16	0.09 ± 0.12	−25.50 ± 0.16
UnTHCPSi-ETH	183.82 ± 0.15	0.07 ± 0.16	10.00 ± 0.15

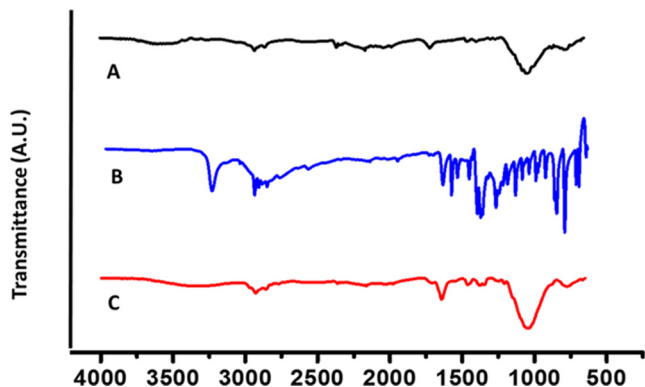


Fig. 1. Attenuated total reflection-FTIR spectra of UnTHCPSi NPs (A), ETH (B), and UnTHCPSi-ETH NPs (C). The acquired spectrum for the ETH-conjugated NPs confirmed the chemical conjugation of ETH onto the PSi NPs

Fabrication of NPs with great stability and security, plummy drug release profiles and useful cellular uptake still represent the main challenges for the progress of NPs with high potential to be

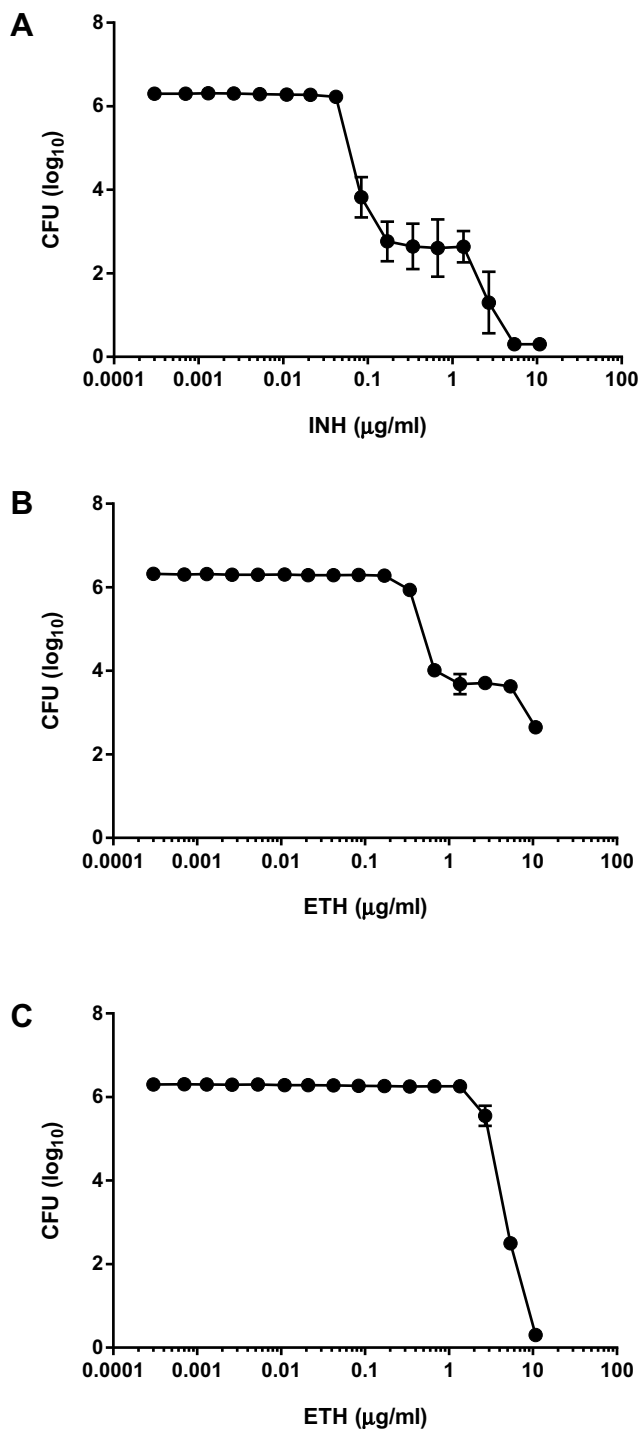


Fig. 2. Evaluation of the antimicrobial effect against *M. tuberculosis* H37Rv. Cultures of *M. tuberculosis* H37Rv were incubated with increasing concentrations of INH (A), ETH (B) or UnTHCPSi-ETH (C). After 7 days of incubation, CFU were performed to determine the bacterial viability. Following ASTM guidelines, the reported value for the limit of detection for microbiological purposes should be “less than the dilution value” if no colonies are recovered; therefore, the limit of detection for our experiments is 1 log₁₀ CFU/mL. All countable colonies, even those below the countable range, were counted and reported as an estimated count. The minimal inhibitory concentration (MIC) of each drug was determined as the lowest concentration of antibiotic that inhibits the growth of a microorganism

applied in nanomedicine. Nevertheless, we have recently published promising results on the potential of the UnTHCPSi NPs for drug delivery.^{20–22} In the present study, 1-ethyl-3-(3-dimethylaminopropyl)carbodiimide (EDC)/N-Hydroxysuccinimide (NHS) coupling chemistry was used to conjugate ETH to the surface of bare particles in an aqueous solution (Table 1 and Fig. 1).²⁷ To functionalize the surface of the particles with ETH, the carboxyl groups of the NPs were activated and covalently conjugated to the amine groups of ETH to form UnTHCPSi-ETH nanocomposites.²⁷

We also set out to compare the in vitro antimicrobial effect of UnTHCPSi-ETH and bare UnTHCPSi against *M. tuberculosis* H37Rv (Trudeau Institute Mycobacterial Collection; Fig. 2).²⁸

The antimicrobial effects of the compounds were determined using an adapted version of the protocol described by Martin et al.²⁷ Briefly, a serial of 2-fold dilutions of the test material (ETH; encapsulated ETH; and the broad-spectrum antibiotic INH as a positive control) were performed. To each well 5×10^5 CFU of *M. tuberculosis* H37Rv was added and the plates were incubated at 37 °C for 7 days. A serial of 10-fold dilutions of the suspensions were plated on nutrient 7H11 and bacterial colony counts were performed after 3 weeks of incubation at 37 °C.

As shown in Fig. 2, INH required lower concentrations to inhibit bacterial growth by half (Fig. 2A, IC₅₀: 0.08066 µg/mL) when compared to ETH (Fig. 2C, IC₅₀: 4.920 µg/mL) and UnTHCPSi-ETH (Fig. 2B, IC₅₀: 4.785 µg/mL). ETH shows better bacterial growth inhibition at the concentration range of 0.5–5 µg/mL and this is comparable to a recent study, in that growth of *M. tuberculosis* H37Rv at different concentrations of ETH were tested, and the best profile was ranging between 0.31 and 5.0 µg/mL.²⁹ Interestingly, within the range of concentrations tested, ETH alone was not able to completely inhibit *M. tuberculosis* growth, as observed in the presence of UnTHCPSi-ETH. These results suggest that the nature of the ETH-loaded NPs synergy is likely due to the weakening of the bacterial cell wall that improves the conjugate penetration. Our in vitro results justify the study of this conjugate in animal models of TB in order to establish whether the antimicrobial effect of the UnTHCPSi-ETH also occurs in vivo.

Acknowledgments

NV thanks Fundação para a Ciência e Tecnologia (FCT, Portugal) and FEDER (European Union) for funding through UID/MULTI/04378/2013, project grant IF/00092/2014 and IF2014 position. Thanks are also due to “Comissão de Coordenação e Desenvolvimento Regional do Norte (CCDR-N)/NORTE2020/

Portugal 2020” for funding through project DESignBIOTechHealth (ref. Norte-01-0145-FEDER-000024). H.A.S. acknowledges financial support from the Academy of Finland (decision nos. 252215 and 281300), the University of Helsinki Research Funds, the Biocentrum Helsinki, and the European Research Council under the European Union's Seventh Framework Programme (FP/2007–2013, Grant No. 310892). The content is solely the responsibility of the authors and does not necessarily represent the official views of the FCT or CCDR-N.

References

1. Siegel RL, Miller KD, Jemal A. *CA Cancer J Clin.* 2015;65:5.
2. Hait WN. *Nat Rev Drug Discov.* 2010;9:253.
3. Laurenzo D, Mousa SA. *Acta Trop.* 2011;111:5.
4. Bollela VR, Namburete EI, Feliciano CS, Macheque D, Harrison LH, Caminero JA. *Int J Tuberc Lung Dis.* 2016;20:1099.
5. Palomino JC, Martin A. *Antibiotics.* 2014;3:317.
6. Banerjee A, Dubnau E, Quemard A, et al. *Science.* 1994;263:227.
7. Johnsson K, King DS, Schultz PG. *J Am Chem Soc.* 1995;117:5009.
8. Baulard A, Betts JC, Engohang-Ndong J, et al. *J Biol Chem.* 2000;275:28326.
9. Francois AA, Nishida CR, Montellano PO, Phillips IR, Shephard EA. *Drug Metab Disp.* 2009;37:178.
10. DeBarber AE, Mdluli K, Bosman M, Bekker LG, Barry CE. *Proc Natl Acad Sci USA.* 2000;97:9677.
11. Vilchère C, Weisbrod TR, Clen B, et al. *Antimicrob Agents Chemother.* 2005;49:708.
12. Dodge AG, Richman JE, Johnson G, Wackett LP. *Appl Environ Microbiol.* 2006;72:7468.
13. Dover LG, Alahari A, Grattraud P, et al. *Antimicrob Agents Chemother.* 2007;51:1055.
14. Hanouille X, Wieruszkeski JM, Rousselot-Pailley P, et al. *J Antimicrob Chemother.* 2006;58:768.
15. Hanouille X, Wieruszkeski JM, Rousselot-Pailley P, Landrieu I, Baulard AR, Lippens G. *Biochem Biophys Res Commun.* 2005;331:452.
16. Jenner PJ, Ellard GA, Gruer PJK, Aber VR. *J Antimicrob Chemother.* 1984;13:267.
17. Vanneli TA, Dykman A, Ortiz de Montellano PRJ. *Biol Chem.* 2002;277:12824.
18. Vale N, Gomes P, Santos HA. *Curr Drug Metab.* 2013;14:151.
19. Vale N, Mäkilä E, Salonen J, Gomes P, Hirvonen J, Santos HA. *Eur J Pharm Biopharm.* 2012;81:314.
20. Shahbazi M-A, Almeida P, Mäkilä EM, et al. *Macromol Rapid Commun.* 2014;35:624.
21. Shrestha N, Araújo F, Shahbazi M-A, et al. *Adv Funct Mater.* 2016;26:3405.
22. Correia A, Shahbazi M-A, Mäkilä E, et al. *ACS Appl Mater Interfaces.* 2015;7:23197.
23. Procedure manual “Colorimetric Redox-Indicator (CRI)” by Anandi Martin and Juan Carlos Palomino; 2012. <<http://tbevidence.org/resourcecenter/sop-package-inserts/>>.
24. Santos HA, ed. *Porous Silicon for Biomedical Applications.* Elsevier; 2014.
25. Santos HA, Hirvonen J. *Nanomedicine.* 2012;7:1281.
26. Santos HA, Mäkilä E, Airaksinen AJ, Bimbo LM, Hirvonen J. *Nanomedicine.* 2014;9:535.
27. Almeida P, Shahbazi M-A, Mäkilä E, et al. *Nanoscale.* 2014;6:10377.
28. Cruz A, Torrado E, Carmona J, et al. *Vaccine.* 2015;33:85.
29. Grau T, Selchow P, Tigges M, et al. *Antimicrob Agents Chemother.* 2012;56:1142.